BMB
reports

BMI-1026 treatment can induce SAHF formation by activation of Erk1/2

*Hyun-Joo Seo, Hye Jeong Park, Hyung Su Choi, So-Yoon Hwang, Jeong-Soo Park & Yeon-Sun Seong**
Department of Biochemistry, College of Medicine, Dankook University, Cheonan 330-714, Korea

BMI-1026 is a synthetic aminopyrimidine compound that targets cyclin dependent kinases (cdks) and was initially designed as a potential anticancer drug. Even though it has been well documented that BMI-1026 is a potent cdk inhibitor, little is known about the cellular effects of this compound. In this study, we examined the effects of BMI-1026 treatment on inducing premature senescence and then evaluated the biochemical features of BMI-1026-induced premature senescence. From these experiments we determined that BMI-1026 treatment produced several biochemical features of premature senescence and also stimulated expression of mitogen activated protein kinase (MAPK) family proteins. BMI-1026 treatment caused nuclear translocation of activated Erk1/2 and the formation of senescence associated heterochromatin foci in 5 days. The heterochromatin foci formation was perturbed by inhibition of Erk1/2 activation. [BMB reports 2008; 41(7): 523-528]

INTRODUCTION

After a given finite number of replications, normal human diploid fibroblasts (HDFs) cease to divide and enter a replicatively arrested state called replicative senescence (1). In replicative senescence the shortened telomere activates the DNA-damage checkpoint kinase pathway, which results in cell cycle progression arrest by inhibiting cdks (2-5). Although telomere erosion can induce the DNA damage response pathway-activated cell cycle arrest, senescence is not a simple end result of telomere shortening. The cumulative influences of other factors are required for launching the senescence program. The other type of senescence called "premature senescence" is triggered by activation of cellular oncogenes, reactive oxygen species, DNA damages and exposure to cytotoxic stress, and/or various kinds of toxic compounds (6,7). Senescence is believed to be one of the defense mechanisms that protect normal cells from tumorous change (8). The senescent cell displays typical phenotypes including absence of mitosis, enlarged flattened morphology, increased senescence associated β-galactosidase (SA-β-gal) activity, and the formation of a distinct chromatin structure known as senescence associated heterochromatin foci (SAHF) (9,10). Except for the fact that the chromatin remodeling machinery and histone chaperones participate in SAHF formation, the signaling pathway and mechanisms of SAHF formation are still under investigation (11). BMI-1026 is an aminopyrimidine compound, which was synthesized in an attempt to discover anticancer drugs that target cyclin dependent kinases (12, 13). *In vitro* kinase assays have determined that BMI-1026 potently inhibits cdk1, cdk2 and cdk5 at nanomolar concentrations, while no effects on other kinases including Erk1, PKCδ, PKA, Plk1, and Aurora A have been observed (12). Even though it has been well documented that BMI-1026 is a potent cdk inhibitor, very little work has been done to examine the cellular effects of BMI-1026 treatment. In this study, the effects of BMI-1026 treatment on inducing premature senescence were examined and the characteristics of the premature senescence phenotype resulting from BMI-1026 treatment were evaluated. Although a multitude of factors can cause senescence, which is the outcome of premature senescence or inhibition of cell cycle progression, the cause and effect relationships between complex features of senescence and direct inhibition of cdk is still unclear. Here, we report that BMI-1026 treatment activated Erk1/2 and induced both SAHF formation and premature senescence in HDFs.

RESULTS AND DISCUSSION

Sub-lethal treatment can induce SA-β-gal activities and caveolin-1 expression

Young HDF cells were treated with 50 nM, 100 nM, and 200 nM concentrations of BMI-1026 for the indicated time periods. As a negative control, HDF cells were treated with dimethyl sulfoxide (DMSO) alone. In HDF cells treated with 100 nM and 200 nM BMI-1026, population doubling was not observed. Since increased SA-β-gal activity is a characteristic marker observed in senescence cells (9), we examined the influence of BMI-1026 treatment on SA-β-gal activity. Around 40% of cells treated with BMI-1026 showed increased SA-β-gal activity, and these increases occurred in a concentration and time depend-

*Corresponding author. Tel: 82-41-550-3875; Fax: 82-41-550-3905; E-mail: seongys@dku.edu

Received 30 April 2008, Accepted 21 May 2008

Keywords: BMI-1026, cdk, Erk1/2, Senescence associated heterochromatin foci (SAHF)

ent manner (Fig. 1A and B), whereas the negative control showed no change in activity. In addition, cells that were treated with 200 nM BMI-1026 showed more SA-β-gal activities than those treated with 100 nM, however, a large number of apoptotic cells were also observed (Fig. 1A). We then examined the changes of other senescence markers including caveolin-1, and transglutaminase 2 (14-16). BMI-1026 treatment (50 nM and 100 nM) induced the accumulation of caveolin-1 within 4 days (Fig. 1C), but accumulation of transglutaminase 2 was not observed, indicating that the accumulation of this protein is a secondary result of senescence and is not directly related with the inhibition of cdks. However the status of caveolin-1 is closely related with the inhibition of cdks. BMI-1026 treated cells showed cell cycle progression arrest at G2/M phase (Fig. 1D). As no mitotic cells were observed, the cells were arrested in G2 phase prior to mitosis.

BMI-1026 treatment can activate MAPK family of proteins

It has been well documented that elevated mitogenic signals (overexpression of ras, raf, and MEK) induce cellular senescence,

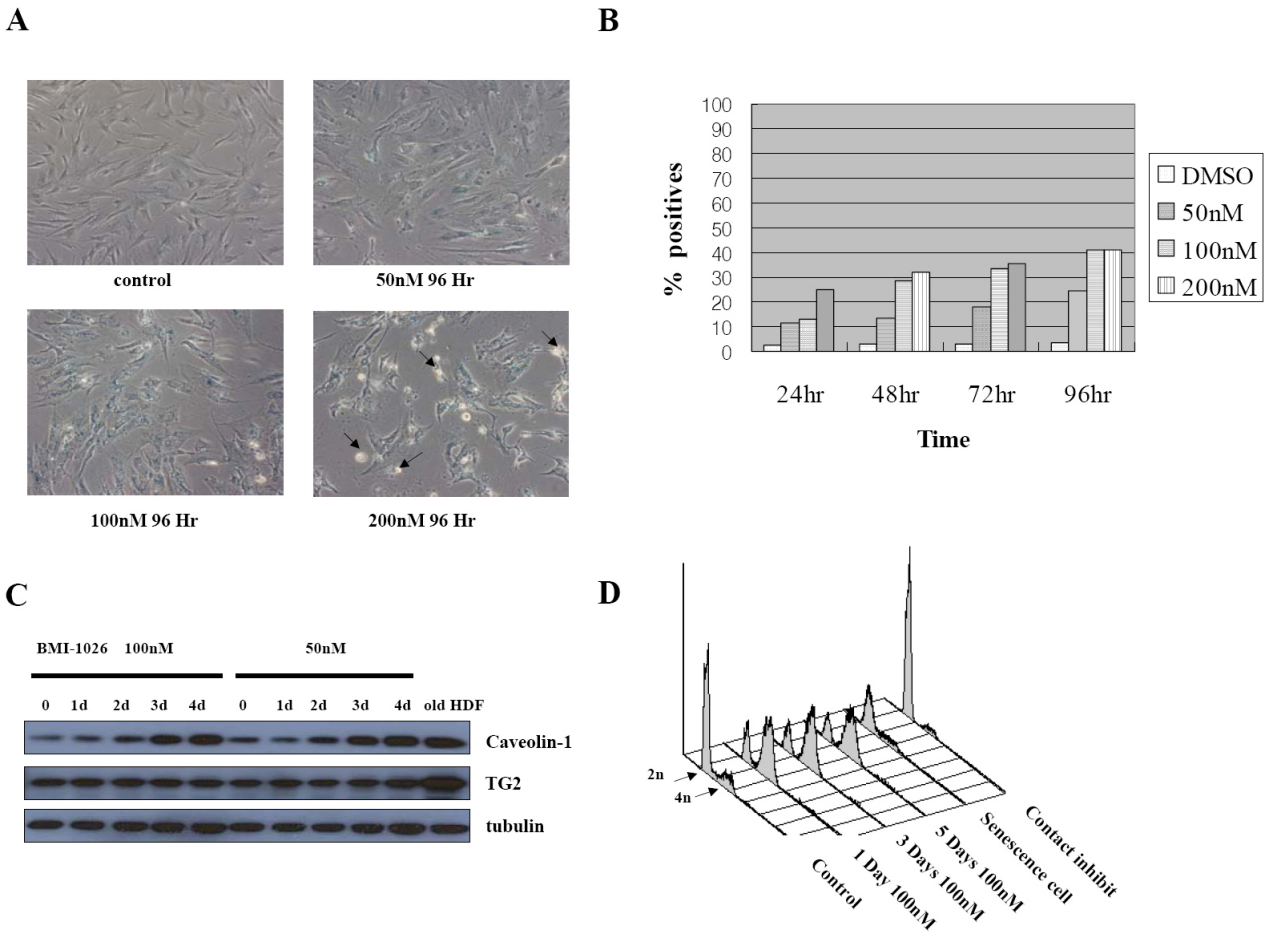

Fig. 1. Administration of sub-lethal doses of BMI-1026 induces a premature senescence like change in HDF cells. (A) HDF cells were treated with 50 nM, 100 nM, and 200 nM concentrations of BMI-1026 for the indicated time period and SA-β-gal activity staining was conducted. Images of cells after BMI-1026 treatment for the indicated time period. As a control we treated cells with DMSO in which did not contain BMI-1026. The arrows in the 200 nM sample represent apoptotic cells. (B) The numbers of SA-β-gal positive cells were quantified at each concentration and the duration after counting approximately 500 cells from more than 10 randomly chosen fields (10 x magnification) were quantified. The data is presented as percentage (C). Expression analysis of caveolin-1 and transglutaminase 2 (TG2). After treatment of the HDF cells with 50 nM or 100 nM BMI-1026 for the indicated time, the cells were lysed, electrophoresed, and immunoblotted with the indicated antibodies. (D) Alteration of cell cycle progression of HDF cells by treatment with BMI-1026 was determined. To examine the effect of BMI-1026 on cell cycle progression, asynchronously growing HDF cells were treated with 100 nM BMI-1026. At the indicated time points, cells were harvested and subjected to flow-cytometry and compared with DMSO treated cells (control), senescence cells, and cells that were arrested in the G1 phase by contact inhibition (Contact inhibit). Arrows indicate the size of the FL2 area representing 2N and 4N DNA content.

and the activity of Erk1/2 increases in the course of ras or MEK induced senescence (17-19). Therefore, we examined the phosphorylation of Erk1/2 and representative MAPK family pathway molecules including MEK, p38 MAPK, and SAPK/JNK in BMI-1026 treated HDF cells. Direct inhibition of cdks by BMI-1026 resulted in the activation of Erk1/2, p38 MAPK, and SAPK/JNK (Fig. 2A). In addition, phosphorylation of Erk1/2 and SAPK/JNK persisted for up to 5 days, whereas phosphorylation of p38 MAPK decreased after 3 days. Although, the decreased level was still higher than that of untreated young cells. Activation of the MAPK family pathway by BMI-1026 treatment was quite different from a recent report which examined the effect of flavopiridol, one of most widely studied cdk inhibitor. In this study flavopiridol treatment was shown to eliminate MAPK family pathway activation upon the treatment of TNF (20).

Immediate changes in Erk1/2 and p38 MAPK phosphorylation, and the effects of MEK inhibitor on Erk1/2 phosphorylation

Since BMI-1026 treatment elicited prolonged phosphorylation of Erk1/2 and p38 MAPK, we wanted to determine the immediate effects of BM-1026 on these proteins. To eliminate serum induced non-specific phosphorylation of MAPKs, we cultivated HDF cells in serum free media for 24 h prior to treatment with BMI-1026. Treatment with BMI-1026 triggered phosphorylation of Erk1/2 and p38 MAPK in a biphasic pattern (Fig. 2B). The early phase activation of Erk1/2 and p38 MAPK was also observed in DMSO treated control cells (data not shown). The second sustained activation of Erk1/2 and p38 MAPK, which was not observed in DMSO treated cells, occurred within 3 h and persisted for 24 h. Since phosphorylation of Erk1/2 can be triggered by activation of MEK, we wanted to determine whether the MEK1 inhibitor, U-0126, could suppress BMI-1026 induced phosphorylation of Erk1/2 (21). Pretreatment with 10 μM U-0126 did suppress the phosphorylation of Erk1/2 to a basal level; however, it did not completely eliminate phosphorylation (Fig. 2C). It is unclear why Erk1/2 is activated by treatment of BMI-1026, but our results suggest that upstream kinase activities may activate Erk1/2 proteins under a state of direct inhibition of cdks.

BMI-1026 treatment induces translocation of activated Erk1/2 and SAHF formation

To convey an activated mitogenic signal to the nucleus, nuclear translocation of activated Erk1/2 is essential (22). In terminally replicative senescent HDFs the nuclear Erk1/2 activities are significantly impaired upon mitogenic stimuli (23). We conducted phospho-Erk1/2 immunofluorescence staining to determine whether activated Erk1/2 could migrate to the nucleus. The phosphorylated Erk1/2 accumulated in the nuclear membrane region after the first day of treatment, and then began to translocate to the nucleus on the third day (Fig. 3). Surprisingly, BMI-1026 treatment induced SAHF formation on the fifth day, and the occurrence of SAHF coincided with the appearance of a prominent nuclear localization signal of

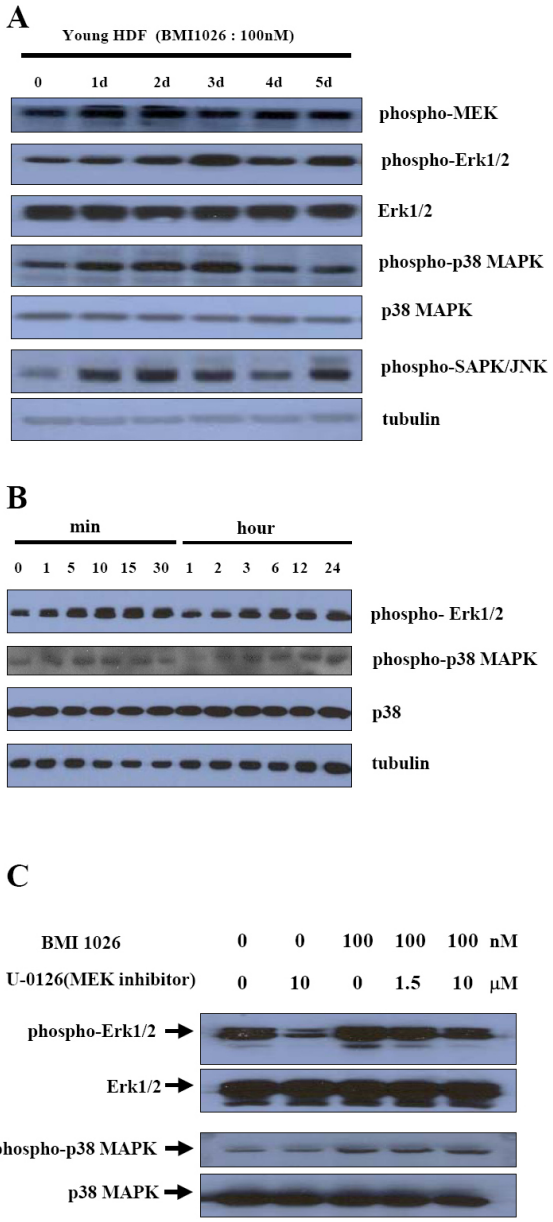

Fig. 2. BMI-1026 treatment can activate the MAP kinase pathway. (A) HDF cells were treated with BMI-1026 at a concentration of 100 nM for the indicated time period. The cell lysates were then electrophoresed and immunoblotted for MAP Kinase family protein activation. (B) Early changes in phospho-Erk1/2 and phospho-p38 MAPK proteins after treatment with BMI-1026. BMI-1026 mediated activation of Erk1/2 and p38 within 3 h of treatment. After 24 h of serum deprivation, HDF cells were treated with 100 nM BMI-1026 for the indicated period. The cell lysates were then electrophoresed and immunoblotted for the detection of phospho-Erk1/2 and phospho-p38 protein. (C) Inhibition of MEK-1 by U-0126 suppressed the activation of Erk1/2. Inhibition of MEK by U-0126 suppressed Erk1/2 phosphorylation. HDF cells were pretreated with U-0126 for 6 h in a serum-containing medium and then treated with BMI-1026 for 24 h. Cell lysates were harvested and immunoblotted for detection of the indicated proteins.

activated Erk1/2. DMSO treatment did not induce SAHF formation. SAHF formation was observed in more than 40% of the cells after 5 days of BMI-1026 treatment and the intensity of SAHF was enhanced with prolonged treatment. Although SAHF occurred after 5 days of BMI-1026 treatment, BMI-1026 treated cells could re-enter the cell replication cycle after removal of the compound, which was also resulted in the disappearance of SAHF (Fig. 3). To investigate whether Erk1/2 activation by BMI-1026 treatment is responsible for SAHF formation, young HDF cells were treated simultaneously with BMI-1026 and U-0126 for 1 week and the numbers of cells with SAHF were determined. Inhibition of MEK by U-0126 perturbed BMI-1026 induced SAHF formation (Table 1). The SAHF formation by treatment of BMI-1026 was closely related with activation and nuclear translocation of Erk1/2, indicating that activated Erk1/2 may potentially collaborate with histone chaperones or chromatin-remodeling machinery for senescence related chromatin modification (11).

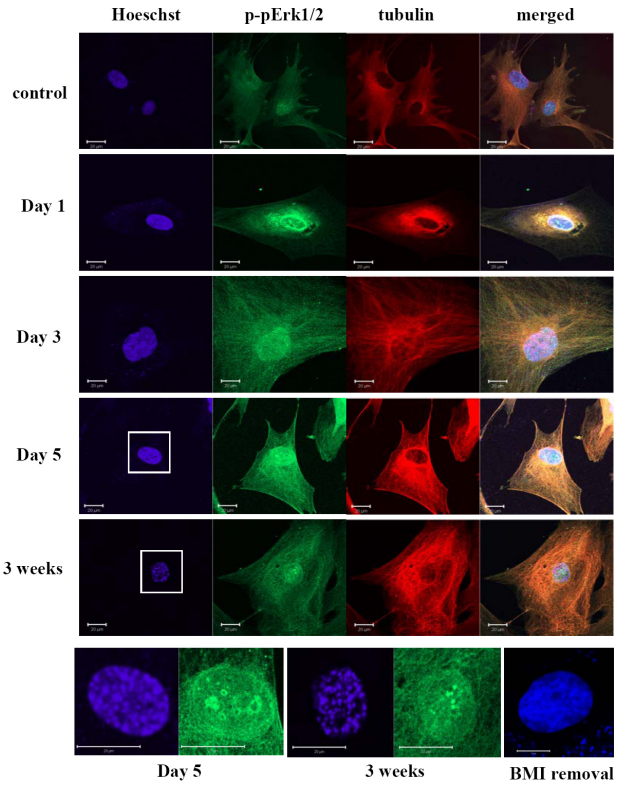

Fig. 3. Nuclear translocation of activated Erk1/2 and SAHF formation by BMI-1026 treatment. After treatment with BMI-1026 for the indicated time period, cells were fixed in 3.7% formaldehyde and then permeabilized with 0.5% Triton X-100 for 5 min prior to incubation with phospho-Erk1/2 (p-pErk1/2) and tubulin antibodies. Hoechst 33452 dye was used for nuclear chromatin staining. The boxed area contains magnified images of representative SAHF formation. BMI-1026 was removed after 1 week of treatment and cells were cultured for an additional 5 days. The white bar in each picture represents 10 μm.

Based on these results we can conclude that direct inhibition of cdks by BMI-1026 treatment can produce premature senescence, including activation of SA-β-gal, accumulation of caveolin-1, activation of Erk1/2 kinase pathway and formation of SAHF. BMI-1026 induced SAHF formation via activation of Erk1/2 is the first experiment to demonstrate that a cdk inhibitor can induce SAHF formation, thus BMI-1026 may be a useful compound for the study of senescence related chromatin dynamics. In addition, since senescence is known barrier to cancerous transformation and given that cancer cells which develop from senescent cells commonly show retarded proliferation (8), direct inhibition of cdks may still represent a promising anticancer therapeutic approach via the induction of senescence and suppression of rapid proliferation.

MATERIALS AND METHODS

Cell culture and BMI-1026 treatment

HDFs were maintained in Dulbecco's modified Eagle's medium (DMEM; Invitrogen, Carlsbad, CA) supplemented with 10% fetal bovine serum (Invitrogen), 100 units/ml penicillin and streptomycin (Invitrogen) in a humidified 5% CO_2 incubator at 37°C. For the experiments, young cells were defined as those that were from less than 30 population doublings (PD), and old cells as those that were obtained from more than 70 PD. Old cells were confirmed by their delayed population doubling times and SA-β-gal staining. Young HDF cells were seeded at a concentration of 1.2×10^4 cells/cm^2 in culture dishes (SPL Life Science, Korea). BMI-1026 (2000x concentrate) dissolved in DMSO was added to the cells 24 h after seeding. Control cells were treated with the same volume of DMSO at the same time interval.

SA-β-gal staining

BMI-1026 treated or DMSO treated cells were stained as previously described (9). Briefly, cells were washed twice with Dulbecco's phosphate buffered saline (DPBS; JBI, Korea) and

Table 1. The inhibition of Erk1/2 by U-0126 can suppress BMI-1026 induced SAHF formation

Types of treatment	%	SAHF cell/Total cell[a]
U-0126 only	0.0	0/220
BMI 50 nM	8.6	45/521
BMI 75 nM	24.1	130/539
BMI 100 nM	41.6	224/539
BMI 50 nM + U-0126	0.6	2/325
BMI 75 nM + U-0126	13.4	36/268
BMI 100 nM + U-0126	27.6	73/262

[a]BMI-1026 (50 nM, 75 nM, or 100 nM) and U-0126 (10 μM) were administrated to young HDF cells simultaneously for 1 week. After fixation and permeabilization, chromatin staining with Hoeschst 33452 was carried out, and the numbers of SAHF forming cells were counted.

then fixed with 3.7% formaldehyde in DPBS for 5 min. After being washed, the cells were stained overnight at 37°C with a solution of 5-bromo-4-chloro-3-indolyl β-D-galactoside (X-gal) containing 1 mg/ml X-gal, 40 mM sodium citrate buffer (pH 6.0), 5 mM potassium ferrocyanide, 5 mM potassium ferricyanide, 150 mM NaCl, and 2 mM $MgCl_2$. The stained cells were then observed and photographed using an Olympus IX 70 microscope equipped with a digital camera.

Flow cytometry

For cell cycle analysis, BMI-1026 treated cells were harvested and fixed with 70% ethanol at -20°C for more than 4 h and then the nuclei was stained with propidium iodide. Cellular DNA was analyzed by fluorescence-activated cell sorting (FACS) using a BD FACSCalibur (Becton Dickinson, San Jose, CA) according to manufacturer's instructions. Data was analyzed using CellQuestPro™ software (Becton Dickinson).

Western blot

BMI-1026 treated HDF cells were washed with cold DPBS (JBI) and directly lysed by boiling for 5 min in sodium dodecyl sulfate-polyacrylamide gel electrophoresis (SDS-PAGE) sample buffer consisting of 50 mM Tris-Cl (pH 6.8), 100 mM dithiothreitol, 2% SDS, 0.001% bromophenol blue, and 10% glycerol. Each cell lysate was subjected to SDS-PAGE and then transferred onto a nitrocellulose membrane (Amersham, Piscataway, NJ). The following primary antibodies were used for immunoblotting analysis: anti-caveolin-1 antibody (clone 2297, BD Transduction Laboratory, Lexington, KY), anti-transglutaminase 2 antibody (ab21258, Abcam, Cambridge, UK), anti-p53 antibody (SC-126, Santa Cruz Biotechnology, Santa Cruz, CA), anti-phospho MEK 1/2 antibody (Ser217/221, #9121, Cell Signaling Technology, Danvers, MA), anti-phospho Erk1/2 antibody (Thr202/Tyr204, #9121, Cell Signaling Technology), anti-phospho SAPK/JNK (Thr180/Tyr182, #9251, Cell Signaling Technology), anti-phospho p38 antibody (Thr180/Tyr182, #9211, Cell Signaling Technology) and anti-α-tubulin antibody (T-5168, Sigma-Aldrich, St. Louis, MO). Horseradish peroxidase (HRP)-conjugated goat anti-rabbit or anti-mouse antibodies (SC-2004, SC-2005, Santa Cruz Biotechnology) were used as secondary antibodies.

Immunofluorescence staining

HDF cells were plated onto poly-D lysine (P0899, Sigma-Aldrich) coated glass coverslips. BMI-1026 was then added at the indicated time periods and concentrations. For immunofluorescence staining, cells were fixed with 3.7% formaldehyde for 5 min and then permeabilized with 0.5% Triton X-100 in DPBS for 5 min. After blocking with 5% bovine serum albumin (BSA), coverslips were incubated with a phospho-Erk1/2 antibody (Cell Signaling Technologies, 1:200) and a α-tubulin antibody (Sigma-Aldrich; 1:500) in a humidified chamber for 2 h. After washing with DPBS containing 1% BSA, the coverslips were incubated with Alexa-488 labeled anti-rabbit antibodies (BD Pharmingen, San Diego, CA; 1:200) and Texas Red conjugated anti-mouse antibodies (Jackson ImmunoResearch Laboratories, West Grove, PA; 1:200). For chromatin visualization, cells were stained with Hoechst 33452 (Sigma-Aldrich; 10 μg/ml). Immunofluorescence stained samples were imaged using a LSM 510 META™ confocal microscope (Carl Zeiss, Thornwood, NY).

Acknowledgements

This study was funded by Medical Science Institute of Dankook University in 2005.

REFERENCES

1. Hayflick, L. and Moorhead, P. S. (1961) The serial cultivation of human diploid cell strains. *Exp. Cell Res.* **25**, 585-621.
2. Harley, C. B., Futcher, A. B. and Greider, C. W. (1990) Telomeres shorten during ageing of human fibroblasts. *Nature* **345**, 458-460.
3. Allsopp, R. C., Vaziri, H., Patterson, C., Goldstein, S., Younglai, E. V., Futcher, A. B., Greider, C. W. and Harley, C. B. (1992) Telomere length predicts replicative capacity of human fibroblasts. *Proc. Natl. Acad. Sci.* **89**, 10114-10118.
4. d'Adda di Fagagna, F., Reaper, P. M., Clay-Farrace, L., Fiegler, H., Carr, P., Von Zglinicki, T., Saretzki, G., Carter, N. P. and Jackson, S. P. (2003) A DNA damage checkpoint response in telomere-initiated senescence. *Nature* **426**, 194-198.
5. Vaziri, H., West, M. D., Allsopp, R. C., Davison, T. S., Wu, Y. S., Arrowsmith, C. H., Poirier, G. G. and Benchimol, S. (1997) ATM-dependent telomere loss in aging human diploid fibroblasts and DNA damage lead to the post-translational activation of p53 protein involving poly(ADP-ribose) polymerase. *EMBO J.* **16**, 6018-6033.
6. Campisi, J. and d'Adda di Fagagna, F. (2007) Cellular senescence: when bad things happen to good cells. *Nat. Rev. Mol. Cell. Biol.* **8**, 729-740.
7. Ben-Porath, I. and Weinberg, R. A. (2005) The signals and pathways activating cellular senescence. *Int. J. Biochem. Cell Biol.* **37**, 961-976.
8. Campisi, J. (2005) Senescent cells, tumor suppression, and organismal aging: good citizens, bad neighbors. *Cell* **120**, 513-522.
9. Dimri, G. P., Lee, X., Basile, G., Acosta, M., Scott, G., Roskelley, C., Medrano, E. E., Linskens, M., Rubelj, I. and Pereira-Smith, O. (1995) A biomarker that identifies senescent human cells in culture and in aging skin *in vivo*. *Proc. Natl. Acad. Sci. USA* **92**, 9363-9367.
10. Narita, M., Nunez, S., Heard, E., Narita, M., Lin, A. W., Hearn, S. A., Spector, D. L., Hannon, G. J. and Lowe, S. W. (2003) Rb-mediated heterochromatin formation and silencing of E2F target genes during cellular senescence. *Cell* **113**, 703-716.
11. Funayama, R. and Ishikawa, F. (2007) Cellular senescence and chromatin structure. *Chromosoma.* **116**, 431-440.
12. Seong, Y. S., Min, C., Li, L., Yang, J. Y., Kim, S. Y., Cao,

X., Kim, K., Yuspa, S. H., Chung, H. H. and Lee, K. S. (2003) Characterization of a novel cyclin-dependent kinase 1 inhibitor, BMI-1026. *Cancer Res*. **63**, 7384-7391.
13. Collins, I. and Garrett, M. D. (2005) Targeting the cell division cycle in cancer: CDK and cell cycle checkpoint kinase inhibitors. *Curr. Opin. Pharmacol*. **5**, 366-373.
14. Park, W. Y., Park, J. S., Cho, K. A., Kim, D. I., Ko, Y. G., Seo, J. S. and Park, S.C. (2000) Up-regulation of caveolin attenuates epidermal growth factor signaling in senescent cells. *J. Biol. Chem*. **275**, 20847-20852.
15. Cho, K. A., Ryu, S. J., Park, J. S., Jang, I. S., Ahn, J. S., Kim, K. T. and Park, S. C. (2003) Senescent phenotype can be reversed by reduction of caveolin status. *J. Biol. Chem*. **278**, 27789-27795.
16. Park, S. C., Yeo, E. J., Han, J. A., Hwang, Y. C., Choi, J. Y., Park, J. S., Park, Y. H., Kim, K. O., Kim, I. G., Seong, S.C. and Kwak, S. J. (1999) Aging process is accompanied by increase of transglutaminase C. *J. Gerontol. A Biol. Sci. Med. Sci*. **54**, B78-83.
17. Serrano, M., Lim, A. W., McCurrach, M. E., Beach, D. and Lowe, S.W. (1997) Oncogenic ras provokes premature cell senescence associated with accumulation of p53 and p16INK1A. *Cell* **88**, 593-602.
18. Lin, A. W., Barradas, M., Stone, J. C., van Aelst, L., Serrano, M. and Lowe, S. W. (1998) Premature senescence involving p53 and p16 is activated in response to constitutive MEK/MAPK mitogenic signaling. *Genes. Dev*. **12**, 3008-3019.
19. Zhu, J. Y., Woods, D., McMahon, M. and Bishop, J. M. (1998) Senescence of human fibroblasts induced by oncogenic Raf. *Genes Dev*. **12**, 2997-3007.
20. Takada, Y., Sethi, G., Sung, B. and Aggarwal, B. B. (2008) Flavopiridol suppresses tumor necrosis factor-induced activation of activator protein-1, c-Jun N-terminal kinase, p38 mitogen-activated protein kinase (MAPK), p44/p42 MAPK, and Akt, inhibits expression of antiapoptotic gene products, and enhances apoptosis through cytochrome *c* release and caspase activation in human myeloid cells. *Mol. Pharmacol*. **73**, 1549-1557.
21. Favata, M. F., Horiuchi, K. Y., Manos, E. J., Daulerio, A. J. Stradley, D. A. Feeser, W. S., Van Dyk, D. E., Pitts, W. J., Earl, R. A., Hobbs, F., Copeland, R. A., Magolda, R. L., Scherle, P. A. and Trzaskos, J. M. (1998) Identification of a novel mitogen inhibitor of mitogen-activated protein kinase kinase. *J. Biol. Chem*. **273**, 18623-18632.
22. Robinson, M. J. and Cobb, M. H. (1997) Mitogen-activated protein kinase pathways. *Curr. Opin. Cell Biol*. **9**, 180-186.
23. Kim-Kaneyama, J. R., Nose, K. and Shibanuma, M. (2000) Significance of nuclear relocalization of ERK1/2 in reactivation of c-fos transcription and DNA synthesis in senescent fibroblasts. *J. Biol. Chem*. **275**, 20685-20692.